Computational model for color mapping on texture images

John H. Xin
Hui-Liang Shen
The Hong Kong Polytechnic University
Institute of Textiles and Clothing
Hong Kong

Abstract. *The interrelationships among spatial distribution in the red, green, and blue channels of texture images of differently woven textile fabrics are investigated. A computational model for color mapping is developed based on the channel proportionality found in the investigation. The computational model developed has two modes: gray-to-color mapping (GCM) and color-to-color mapping (CCM) that deal with different images. For the GCM mode, the spatial distribution of luminance is known. The algorithm needs to deduce data in three channels for a color image from 1-D spatial distribution of luminance. Whereas in the CCM mode, the information for each of the three channels is known. Numerical and psychophysical experiments are carried out to evaluate the accuracy of the color mapping algorithm quantitatively. Satisfactory color accuracy of the mapped images was obtained according to the results of both numerical calculation and visual experiment.* © *2003 SPIE and IS&T.*
[DOI: 10.1117/1.1604395]

1 Introduction

Color mapping on texture images deals with reproducing a texture color image accurately so that it is perceptually close to the original one. Color mapping on texture images should provide an effective way for color texture image coding. It should also provide a way for simulating physical surfaces with color texture information with high color fidelity on a pixel-wise scale. Color mapping with high fidelity is much needed in systems such as computer-aided design for textile fabrics, texture simulation, and visualization. For example, in a traditional fabric design process in which physical samples are produced, the effect of the design using yarns with different colors can only be visualized through the coloration of yarns, followed by weaving or knitting those yarns into fabrics. This is a very time-consuming process. If more colors are going to be used in the design, more coloration and weaving processes need to be carried out. With the technique of color mapping on texture images, one can visualize the final style of the fabrics before they are actually produced.[1] In textile coloration and color quality control along the supply chain of the colored goods, the visualization of solid colors on display devices has become a routine process for many companies.[2] As the final fabric product is textured, there are demands

for the mapping of solid colors to various texture patterns, so that visualization of the final products can be achieved. In these applications and many others, it is very important to simulate texture images with high color accuracy. For textiles and clothing industries in particular, it is generally accepted that pass and fail tolerance for colored goods is about 1.0 to 1.5 CIELAB color difference units. If a method of color mapping cannot achieve this magnitude of color accuracy, it will affect the final displayed samples and in turn will affect color quality judgment.

In the literature of texture image analysis, many researches have been conducted in the domain of texture mapping and synthesis.[3–8] Texture mapping deals with rendering textures to surfaces of 3-D computer graphics to produce natural and realistic effects.[3,4] Texture synthesis generates a new instance of a representative texture sample from the underlying stochastic process of an original texture. The appearance of the generated texture sample should be very close to the original one. Campisi, Neri, and Scarano[5] proposed a method to reproduce a texture perceptually close to a given prototype, according to the assumption that the human visual system is preattentively unable to distinguish textures having the same first- and second-order distributions, but different higher-order distributions.[6] Heeger and Bergen described a method for synthesizing stochastic texture images that match the texture appearance of a given sample using a set of statistical properties.[7] These works emphasized the perceptual similarity of textural effects compared to the original one. Texture information of the reproduced image, on the other hand, may be different from that of the original one. However, in those works, the color accuracy for the reproduced images was not considered. In the colorimetric characterization of low and high-end digital cameras, Hong, Han, and Lou[8] proposed an approach for on-screen texture visualization by assuming that the pixels in the reproduced textile fabric image differed only in luminance and not in chromaticity coordinates.

To address the problem of color fidelity in the color-mapping process, this study emphasized synthesizing a color image that is perceptually close to the physical sample, with a high degree of color accuracy. A corresponding computational model for color mapping on textural images was developed. Using this model, the demands
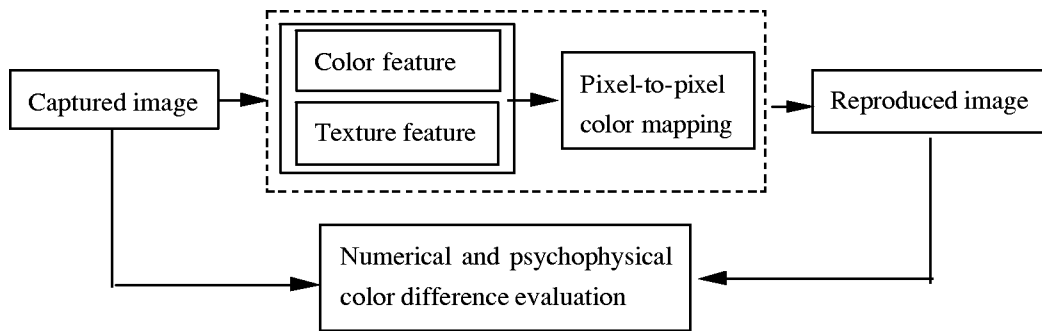
Fig. 1 Color-mapping process adopted in this study with emphasis on color fidelity.

from textile and garment industries toward color accuracy in texture image simulations can be dealt with. The mapping algorithm was driven by a global-to-local analysis of the input textural images, which deals with image data pixel by pixel. The process of image color mapping is shown in Fig. 1. In this color-mapping process, the color and texture features of the image were studied, and the parameters of the algorithm were fine tuned under the guidance of numerical color different evaluation. The images in this study were prepared by scanning the textile fabrics with 16 different texture patterns. Each texture pattern was dyed using five different colors. The most elementary color space, the RGB space, was used in the procedure of color mapping, since it directly corresponds to the input/output signal of imaging devices.[1] The numerical evaluation of the computational model is carried in the $L*a*b*$ (CIELAB) color space, recommended by the International Commission on Illumination[9] in 1976, which is reasonably uniform and has been widely used in color difference calculation.[1]

2 Development of the Color-Mapping Algorithm

Texture images were scanned in using an Epson GT-10000+ flatbed color image scanner. The physical samples were 16 differently woven cotton fabrics. Samples of each of the woven patterns were dyed using reactive dyestuffs into five colors: green, orange, purple, pink, and turquoise blue. All together 80 fabric samples were scanned in a resolution that gave approximately equal visual appearances to those of the physical samples when viewed under normal viewing distances of about 25 to 30 cm. The green texture image samples with different woven patterns are given in Fig. 2.

2.1 Analysis of the Chromaticity Coordinates of Texture Images

As digital imaging devices can only produce RGB digital counts for the texture samples, to study the chromaticity coordinates of a texture image, the imaging devices should be characterized to obtain the device-independent colorimetric values. In the domain of color imaging technology, the method of device characterization has been extensively studied,[10] and it was suggested that the most straightforward RGB to XYZ tristimulus transformation was high-order polynomial regression. Mapping from RGB to XYZ using 11 terms can be represented by Eq. (1).

$$\mathbf{H} = \mathbf{MR},\tag{1}$$

where

$$\mathbf{H} = (X, Y, Z)^T,\tag{2}$$

$$\mathbf{R} = (R, G, B, RG, RB, GB, R^2, G^2, B^2, RGB, 1)^T.\tag{3}$$

The superscript T in Eqs. (2) and (3) stands for vector transpose, and $\mathbf{M}$ is the 3×11 transform matrix that can be resolved by the method of least square fitting.[11] Color standards such as the Macbeth Color Checker Chart and IT8 charts can be used for characterization purposes. To achieve better characterization results, the nonlinear relationship between the device RGB values and their corresponding XYZ values of gray patches on charts was investigated. The nonlinear nature could be adjusted using a 1-D look-up table, and then the linearized RGB values were applied in the polynomial regression instead of the measured RGB values.[8,10]

After the characterization of the imaging device, the RGB values of the pixels were ready to be transformed to the corresponding XYZ values. The XYZ values of a pixel
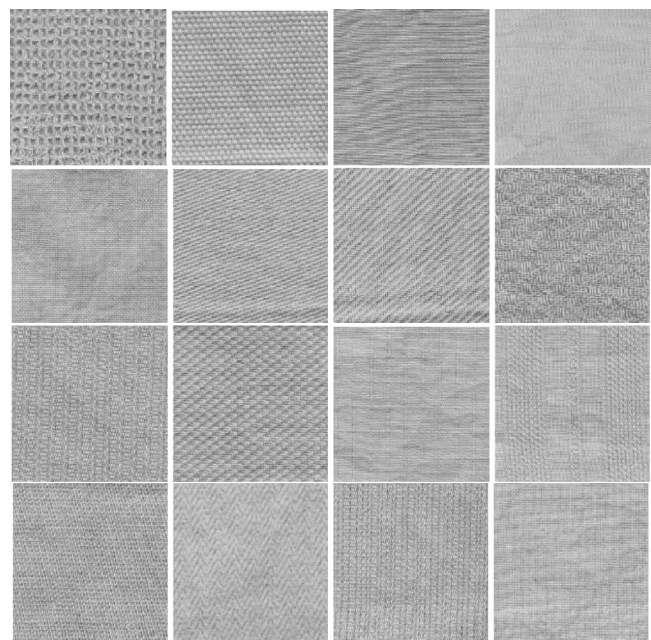

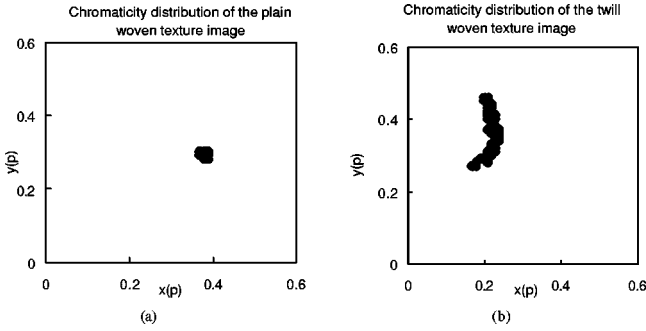**Fig. 2** The 16 different texture images used in this study.

(a)

(b)

Fig. 3 The distribution of chromaticity coordinates for two different texture images: (a) is for plain woven patterns and (b) is for twill woven patterns.
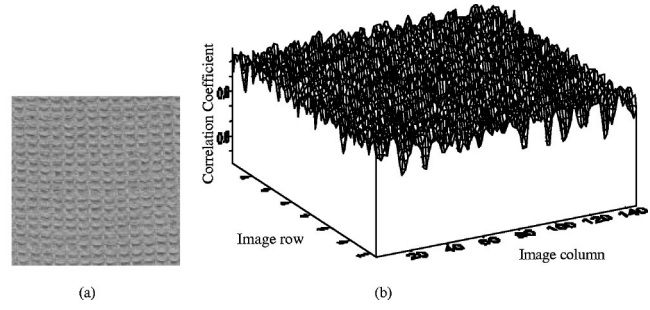

(a)

(b)

Fig. 4 Channel correlation coefficient of one of the texture images studied: (a) the texture image and (b) the correlation coefficient of the green and blue channels.

can be converted to their corresponding luminance Y and chromaticity coordinates x and y following the CIE colorimetry, where

$$x = X/(X+Y+Z), \qquad (4)$$

and

$$y = Y/(X+Y+Z). \qquad (5)$$

Therefore, the vector (x,y,Y) can be used to represent the color of pixels in a texture image. The distribution of the chromaticity coordinates of the pixels of two different texture images of textile fabric samples were plotted in Figs. 3(a) and 3(b) as examples. As seen from Fig. 3(b), the distribution of chromaticity coordinates of the pixels differs significantly. Therefore the assumption of constant chromaticity coordinates adopted by Hong *et al.*[8] has only very limited use to provide accurate color mapping for textile fabrics.

Accuracy of the characterization of the imaging device is highly dependent on the hardware device. Current scanner technology may be unable to support the requirement of textile and clothing applications at an affordable price. In this study, the accuracy of the characterization of an Epson GT-10000+ using the method illustrated was 2.7 CIELAB color difference units using Macbeth Color Checker Chart, and was considered inadequate in achieving the color accuracy requirement. Nevertheless, since the distribution of the chromaticity coordinates for pixels in Figs. 3(a) and 3(b) is a relative term, it is not affected by the absolute accuracy of the scanner characterization.

2.2 Analysis of Channel Distribution

The RGB color space directly corresponds to the output of imaging devices. For a particular pixel p, the RGB signal could be defined as follows:[1]

$$m_n(p) = \int L(\lambda;p)s_n(\lambda)d\lambda, \qquad (6)$$

where $L(\lambda;p)$ refers to the spectral distribution function of the light entering the imaging device at a pixel p, $s_n(\lambda)$ refers to the spectral sensitivity of the appropriate sensor, and n denotes a red, green, or blue channel. For a typical

imaging device, each of the $s_n(\lambda)$ of the red, green, and blue channels has a distribution across a certain range of wavelength, with some degree of overlap between each other. Since $s_n(\lambda)$ is fixed and dependent on the characteristics of the imaging device, $m_n(p)$ is mainly determined by the factor $L(\lambda;p)$. Due to the property of statistical similarity of the textile textures, the light reflected from the texture surface will be confined to a certain range.

The signals produced in the filter array of the imaging devices are not independent but highly correlative, as discussed by other researchers.[12,13] The correlation coefficient between two channels can be calculated by Eq. (7)[12]

$$r_{12}(p) = \frac{S_{12}(p)}{[S_{11}(p) \cdot S_{22}(p)]^{1/2}}, \qquad (7)$$

where

$$S_{12}(p) = \sum_{p' \in N(p)} [m_1(p') - \bar{m}_1][m_2(p') - \bar{m}_2], \qquad (8)$$

$$S_{11}(p) = \sum_{p' \in N(p)} [m_1(p') - \bar{m}_1]^2, \qquad (9)$$

$$S_{22}(p) = \sum_{p' \in N(p)} [m_2(p') - \bar{m}_2]^2, \qquad (10)$$

the $\bar{m}_1$ and $\bar{m}_2$ are the mean values of channels 1 and 2, respectively, and $N(p)$ denotes the neighbor domain of p. As the purpose here is to investigate the local channel correlations, $r_{12}(p)$ was calculated in a 3×3 window around pixel p. In Fig. 4, the channel correlation coefficients for the green and blue channels of the texture image shown were ploted. The correlation coefficients are very high in all pixel positions, ranging from 0.791 to 0.996, with an average value of 0.885. The investigation of the 80 texture images of the textile fabrics confirmed that the average channel correlation coefficients were higher than 0.83, between any two channels. These results indicated highly correlative properties between channels.

Knowing that there are high channel correlations in the texture images studied, the interchannel spatial distribution in pixel scale was further studied. The luminance Y for each
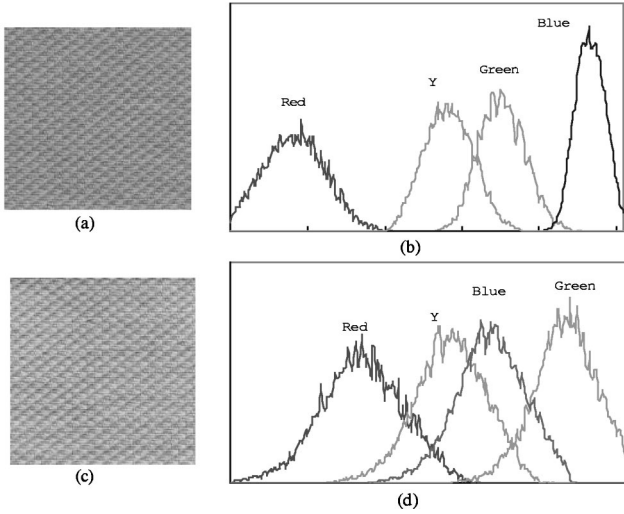
(a)

(b)

(c)

(d)

Fig. 5 Histograms of the red, green, blue, and Y channels: (a) image 1, (b) histograms of image 1, (c) image 2, and (d) histograms of image 2.

Fig. 6 The linear proportionality relationship between Δm_Y and $\Delta m_{\mathrm{green}}$.

pixel was calculated according to the Federal Communications Commission (FCC) RGB color space[1]:

$$Y = 0.299R + 0.587G + 0.114B. \tag{11}$$

The typical histograms of channels red, green, blue, and luminance Y of two texture images are plotted in Fig. 5. It can be seen that the histogram of each channel has similar shapes (only differing in height and width) for the same texture image, which is due to the similarity in the texture spatial distribution and the high channel correlation coefficients.

To study the spatial distribution of the color components more locally, the deviation of pixel p to the mean value in channel n is calculated as the following:

$$\Delta m_n(p) = m_n(p) - \bar{m}_n, \tag{12}$$

where $\bar{m}_n$ is the mean value of channels red, green, blue, or luminance Y. It was found that the relationships between Δm_n of any two different channels were linearly proportional. A typical example of the relationship between $\Delta m_{\mathrm{green}}$ and Δm_Y for an image studied is plotted in Fig. 6. In Fig. 5 for the green and blue colored images, the spatial distribution of channel red is more coarse or noisier than that of the green or blue channels, the width of histogram of the red channel is also wider. When investigating the histograms of the 80 texture images, the same results were found, which indicated that when $\bar{m}_n$ was small, the deviation of the spatial distribution in channel n was relatively large.

2.3 Two Modes of Color Mapping

There are two modes of color mapping according to the different original images under processing. These are gray-to-color mapping (GCM) and color-to-color mapping (CCM). The difference between these two modes is that the spatial distribution available is 3-D in the CCM mode and 1-D in the GCM mode. The important part of the GCM
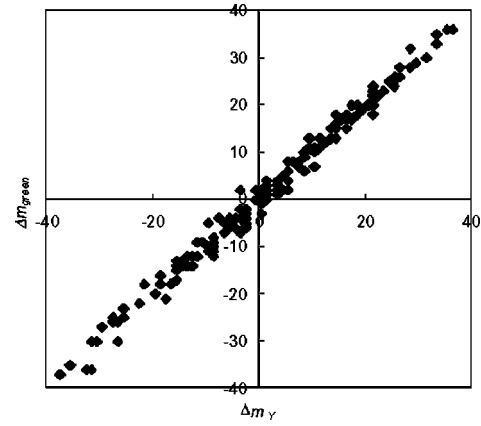
mode is deducing 3-D channel information of red, green, and blue channels from the existing 1-D spatial distribution of brightness or luminance of the original image. The two different modes are discussed in more detail in the following sections.

2.3.1 GCM mode

In the GCM mode, only the mean color $\bar{m}_n$ and spatial distribution of luminance Y are available. All the other information needed in the algorithm is global or statistical, obtained from the histogram analysis.

As discussed in Sec. 2.2, $\Delta m_n(p)$ of different channels are approximately proportional to each other. Based on this relationship, a model of color mapping in the GCM mode is then defined:

$$m_n^G(p) = \bar{m}_n + f^G(\bar{m}_n) \cdot \Delta m_Y(p) + \delta_n^G(p), \tag{13}$$

where the superscript G denotes the GCM mode, $f^G(\bar{m}_n)$ is the proportionality function, and $\delta_n^G(p)$ is the error factor between the reproduced image and the original image in channel n. The goal of color mapping is to decide the appropriate form of function $f^G(\bar{m}_n)$, so that $\delta_n^G(p)$ is minimized.

As the shapes of the histograms of the red, green, and blue channels are quite similar, we can simply use the width of the histogram w_n to represent that histogram. The histogram width w_n here is defined as the minimum distance between the low value T_L and high value T_H that covers a 98% area of the whole histogram of channel n:

$$w_n = \min |T_L - T_H|, \tag{14}$$

where T_L and T_H satisfy

$$\sum_{x=T_L}^{T_H} h_n(x) \Big/ \sum_{x=0}^{255} h_n(x) = 98\%, \tag{15}$$

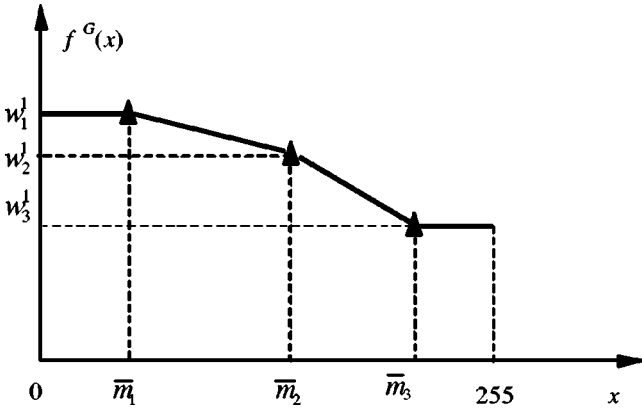and $h_n(x)$ is the distribution of the histogram of channel n.

Fig. 7 The plot of the proportionality function $f^G(x)$.

Considering that w_n may differ widely depending on the properties of the texture in different images, the relative width with respect to the width of the luminance channel w_Y is calculated:

$$w_n^1 = w_n / w_Y. \tag{16}$$

According to the proportionality relationship found, the function $f^G(x)$ can be defined using the global information of the histograms and the mean value $\bar{m}_n$:

$$f^G(x) = \begin{cases} w_1^1 & 0 \leq x \leq \bar{m}_1 \\ \dfrac{w_1^1 - w_2^1}{\bar{m}_1 - \bar{m}_2}(x - \bar{m}_2) + w_2^1 & \bar{m}_1 < x \leq \bar{m}_2 \\ \dfrac{w_2^1 - w_3^1}{\bar{m}_2 - \bar{m}_3}(x - \bar{m}_3) + w_3^1 & \bar{m}_2 < x \leq \bar{m}_3 \\ w_3^1 & \bar{m}_3 < x \leq 255 \end{cases}, \tag{17}$$

where $\bar{m}_1 < \bar{m}_2 < \bar{m}_3$. In the range from $\bar{m}_1$ to $\bar{m}_3$, the function $f^G(x)$ is proportional and linear, while between 0 and $\bar{m}_1$, $\bar{m}_3$ and 255, it is clipped to w_1^1 and w_3^1, respectively. The shape of $f^G(x)$ is plotted in Fig. 7.

Since in the GCM mode the only available information is the mean values and spatial distribution of $m_Y(p)$, the parameters of $f^G(x)$ must also be deduced from $m_Y(p)$. Theoretically, for different texture images, the parameters of $f^G(x)$ should also be different for the accurate description of a particular texture. However, considering the complicated statistical properties of the texture images[14] and the applicability of the algorithm, an empirical form of $f^G(x)$ was thought to be more appropriate for this study, provided that the color accuracy for the textile application could be met.

2.3.2 CCM mode

The CCM mode here can be considered as a special case of the approach. Unlike the GCM mode, the original image in the CCM mode is colored, which means that the 3-D spatial distributions of the original image are known. In the CCM mode, the proportionality function f^C is determined on a

pixel-wise scale, not a global one from the histogram analysis. We modify Eq. (13) accordingly and obtained the following equation:

$$m_n^C(p) = \bar{m}_n + f^C(\bar{m}_n; p) + \delta_n^C(p), \tag{18}$$

where the superscript C denotes the CCM mode. Note that the proportionality term $f^G(\bar{m}_n) \cdot \Delta m_Y(p)$ in Eq. (13) becomes $f^C(\bar{m}_n; p)$, which means that the proportionality function is directly mapped for every pixel. Hence the function f^C becomes:

$$f^C(x; p)$$
$$= \begin{cases} \Delta m_1(p) & 0 \leq x \leq m_1(p) \\ \dfrac{\Delta m_1(p) - \Delta m_2(p)}{m_1(p) - m_2(p)}[x - m_2(p)] + \Delta m_2(p) & m_1(p) < x \leq m_2(p) \\ \dfrac{\Delta m_2(p) - \Delta m_3(p)}{m_2(p) - m_3(p)}[x - m_3(p)] + \Delta m_3(p) & m_2(p) < x \leq m_3(p) \\ \Delta m_3(p) & m_3(p) < x \leq 255 \end{cases}, \tag{19}$$

where $m_1(p) < m_2(p) < m_3(p)$. The shape of $f^C(\bar{m}_n; p)$ is similar to that of $f^G(\bar{m}_n)$ in the GCM mode, despite that it now contains the spatial position p of the image. In the CCM mode, the error factor $\delta_n^C(p)$ in all pixels is 0 when applying the algorithm with the mean color value $\bar{m}_n$ of the original image.

3 Experimental Analysis of the Accuracy of the Models for Color Mapping

Color mappings based on the prior two modes were performed. Both numerical and psychophysical evaluations were undertaken to investigate the effectiveness of the computational model proposed. In an attempt to establish the generic form of $f^G(x)$, all of the 80 fabric samples with 16 different texture patterns were used. The details of those samples and the method of digitizing the samples can be found in Sec. 2. After a fine tuning of parameters based on the investigation of different images, the most suitable empirical equation for the GCM mode was obtained as the following:

$$f^G(x) = \begin{cases} 1.2 & 0 \leq x \leq 64 \\ -\dfrac{0.4}{128}(x - 64) + 1.2 & 64 < x \leq 192 \\ 0.8 & 192 < x \leq 255 \end{cases}. \tag{20}$$

Using the scanner characterization procedure discussed earlier, the RGB values of pixels could be converted to device-independent XYZ values. These XYZ values can then be converted to CIELAB for the calculation of the color difference ΔE_{Lab} between two sets of CIELAB coordinates (L_1^*, a_1^*, b_1^*) and (L_2^*, a_2^*, b_2^*)[9]:

$$\Delta E_{Lab} = [(\Delta L^*)^2 + (\Delta a^*)^2 + (\Delta b^*)^2]^{1/2}, \tag{21}$$

where $\Delta L^* = L_2^* - L_1^*$, $\Delta a^* = a_2^* - a_1^*$, and $\Delta b^* = b_2^* - b_1^*$.
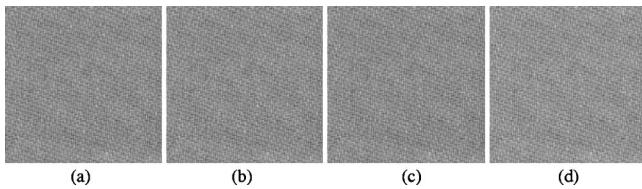
Fig. 8 An example of the color mapping results using GCM and CCM modes: (a) original image, (b) texture information of the original image, (c) color-mapping result with the mean color of the original image in the GCM mode, and (d) color-mapping result with a green solid color in the CCM mode.

In this study, both numerical and psychophysical experiments were employed to evaluate the accuracy of the computational model of color mapping. Detailed descriptions are given in the following.

3.1 Numerical Evaluation

In both GCM and CCM modes, texture images can be mapped with solid color. Figure 8 shows an example of color mapping using the texture information of the original image. In the CCM mode, the reproduced and original images are exactly the same when $\bar{m}_n$ of the original image are applied, and thus the ΔE_{Lab} for every pixel is 0, as can been deduced from the proportionality function of Eq. (19). Thus the numerical experiment was conducted in the case that the luminance channel (containing only texture information) is mapped with the mean color of the original image in the GCM mode. Although the purpose here is to evaluate the performance of the computational model, this technique is also very useful in color texture image coding, since it provides a way to simulate a color texture image, knowing only the texture information and the average color value. Plotted in Fig. 9 are the average pixel-wise ΔE_{Lab} values between the original and reproduced images in the GCM mode. The average ΔE_{Lab} for all 80 samples is 1.29.

It was reported that the threshold for detecting the color difference of a pair of solid color samples is around $1.0 \, \Delta E_{Lab}$.[15] Nevertheless, in the case of color with texture, one can hardly perceive the difference between the original image and the reproduced one, even if the mean color difference is 1.29, as shown in this study. This result may be attributable to the parametric effect of the texture.[16,17] On the other hand, the pixel-by-pixel color difference calculation has shortcomings, as it may not repre-
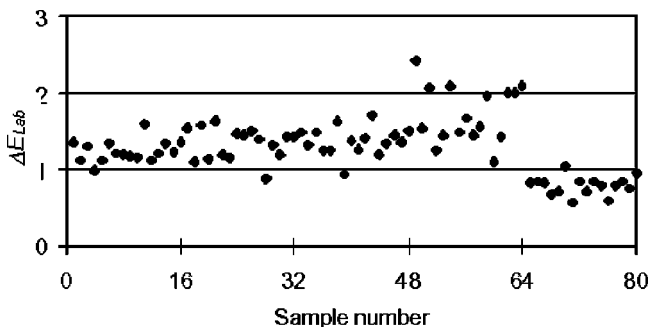
sent the perceived overall color difference. Some method of weighting was used in a previous work.[18] However, in this study, the images used are all texture samples with regular patterns and with no obvious local variance, such as bright or high contrast regions, etc. The pixel-by-pixel color difference calculation is therefore quite reliable.

3.2 Psychophysical Evaluation

While the numerical experiment mainly evaluates pixel-wise accuracy during color mapping, the psychophysical experiment attempts to evaluate the visual difference on color and texture appearance that may exist between the color-mapped texture images and physical samples. The fabric sample was attached on a gray plane standing in a Verivide viewing booth at a illuminating/viewing geometry of 80/0 deg to the normal of the sample plane. A D65 simulator of the viewing booth was properly adjusted to give similar luminance to that of the monitor white point. A texture image was displayed in the center of a 21-in. Sony Trinitron monitor screen adjacent to the viewing booth. The physical sizes of the physical and displayed samples were identical. The gray background of the monitor was adjusted to be equal to that of the gray background supporting the physical samples. A Photo Research spectroradiometer model PR704 was used to measure the colors of both fabric and displayed samples. The procedure of the visual assessment consisted of four steps.

1. Measuring of the fabric samples in the viewing booth to obtain the XYZ values. We characterized the monitor using a gain-offset-gamma (GOG) model,[19] and then converted the XYZ values into the monitor RGB values by the GOG model.
2. Mapping the solid color to the same texture pattern as the fabric sample using the method developed in this study.
3. Measuring the texture image generated on the screen using the spectroradiometer, and calculating the color difference between the texture image and corresponding fabric sample.
4. A panel of ten observers with normal color vision tested by the congenital color vision deficiencies test[20] was invited to evaluate the matching using a seven-point scale. Grade 1 was the worst color matching and grade 7 was the perfect color matching between the texture image on the monitor and the fabric sample in the viewing booth.

The average ΔE_{Lab} in step (1) between the displayed solid colors predicted from the GOG model and the physical sample is 1.10. After mapping the solid color to the texture images, the ΔE_{Lab} was calculated in step 3. These color differences and the visual assessment ratings in step 4 for the 80 samples were plotted in Figs. 10(a) and 10(b), respectively. The average ΔE_{Lab} between the color-mapped texture images and the physical samples is 1.12. This result clearly indicates that color mapping does not introduce additional errors in spectroradiometric measurement, and hence the color-mapping algorithm produces accurate results. It seems that the GOG model still has some errors in predicting displayed color. If this error can be reduced, the
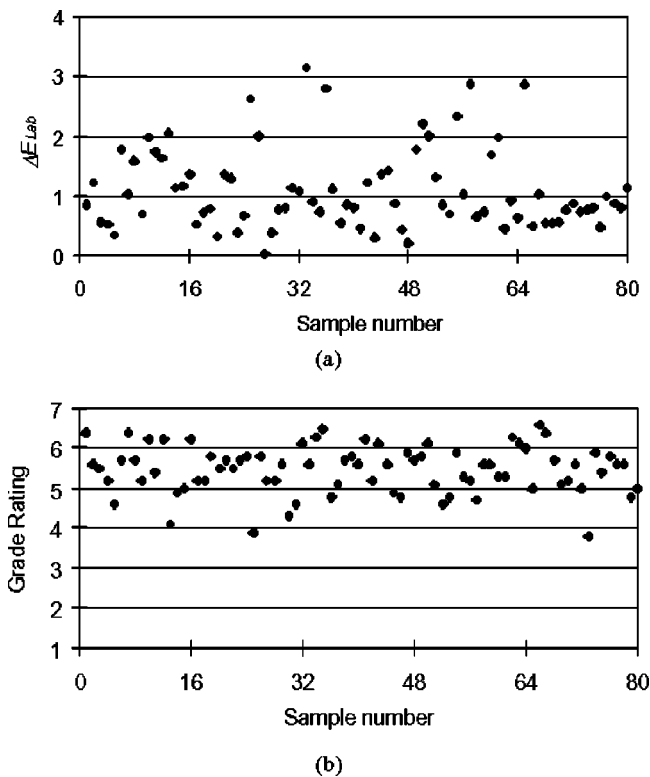

Fig. 9 The average pixel-wise ΔE_{Lab} between the original and reproduced image in the GCM mode.

Fig. 10 Physical and psychophysical evaluation of the CCM mode results: (a) ΔE_{Lab} of the spectroradiometric measurement, and (b) grade rating of the visual assessment.

spectroradiometric measurement results for the color-mapped texture image can be further improved. The average grade of the visual assessment is around 5.5 in a 1 to 7 scale for all of these 80 samples, which indicates that the visual appearance of the simulated samples are quite close to the physical samples. The mean variation between the observers for the visual assessment can be indicated by the coefficient of variation CV,[17] which is equal to 40%. This magnitude of variation is very similar to a previous study on multimedia color appearance matching.[21] Therefore, according to the results of both spectrophotometric measurement and visual assessment, the results of the color mapping were quite accurate. Further analysis on the data showed that there are no obvious relationships between the ΔE_{Lab} value obtained from the spectroradiometric measurements and their corresponding visual grades. The reason for this was considered to be simply because observers tended to hesitate giving the highest rating 7, even though the magnitude of color difference is small. Instead they often gave 5 to 6 to be on the safe side. The other reason might be attributable to the media difference, the physical samples being the reflective medium and the displayed samples being the self-luminous medium, which affects color appearance matching. Nevertheless, the average rating of 5.5 indicates that the accuracy of the color mapping using the model developed in this study was satisfactory.

4 Conclusion

Based on the study of channel correlation and histogram distribution, the proportionality property between channels

is established. A computational model of color mapping on texture images is then established. The color accuracy of the model developed was tested quantitatively using both objective and subjective evaluation methods. Two mapping modes, GCM and CCM, are discussed. The difference between the two modes is due to knowledge of the spatiochromatic information of the original image. The contents of the proportionality functions are different for the two modes. Both GCM and CCM perform well in this study. However, GCM deals with mapping from one to three dimensions, while CCM deals with mapping from three dimensions to three dimensions. CCM is considered to be more reliable when the noise is low. The psychophysical evaluation conducted also shows that the reproduced images satisfactorily match the original samples, which further verifies the effectiveness of the model proposed. Although this study concerns only solid-color textures, it can be extended to multicolor texture images once these images are properly segmented. As the computational model of color mapping is based on the proportionality relationship between channels, it performs well for regular textures, such as textile fabrics. But for textures where the proportionality basis does not hold, such as angular textures with high contrast, the model may fail to produce satisfactory results. In this study, it is also found that due to interreflection within physical texture samples, the color also has an impact on the texture appearances of the scanned images. For example, the pixel variation (or texture contrast) of bright color is usually weaker than that of dark color. This is, however, slightly different from the visual perception. This problem is not addressed in the study, and it is suggested that this effect may be considered in future work.

References

1. S. J. Sangwine and R. E. N. Horne, *The Color Image Processing Handbook*, pp. 67–92, Chapman and Hall, London (1998).
2. J. Xin and R. Lawn, "Digtal swatches—A practical guide," *Intl. Dyer* **186**(11), 28–30 (2001).
3. R. Westermann and B. Sevenich, "Accelerated volume ray-casting using texture mapping," *Visualization VIS'01 Proc.*, pp. 271–278 (2001).
4. A. M. Abbas, L. Szirmay-Kalos, G. Szijarto, T. Horvath, and T. Foris, "Quadratic interpolation in hardware Phong shading and texture mapping," *Spring Conf. Computer Graphics*, pp. 181–188 (2001).
5. P. Campisi, A. Neri, and G. Scarano, "A single input three output model based approach to color texture generation," *1998 Intl. Conf. Image Process.* **1**, 67–71 (1998).
6. B. Julesz and R. Bergen, "Textons, the fundamental elements in pre-attentive vision and perception of textures," *Bell Syst. Tech. J.* **62**, 1619–1645 (1983).
7. D. Heeger and J. Bergen, "Pyramid-based texture analysis/synthesis," *Proc. ACM SIGGRAPH*, pp. 229–238 (1995).
8. G. Hong, B. Han, and M. R. Lou, "Colorimetric characterization of low-end digital camera and its application for on-screen texture visualization," *Proc. Intl. Conf. Image Process.*, pp. 741–744 (2000).
9. Publication CIE, *Colorimetry*, 2nd ed., Central Bureau of the CIE (1986).
10. H. R. Kang, *Color Technology For Electronic Imaging Devices*, SPIE Optical Engineering Press, Bellingham, WA (1996).
11. W. H. Press, S. A. Teukolsky, W. T. Vetterling, and B. P. Flannery, *Numerical Recipes in C: The Art of Scientific Computing*, 2nd ed., Cambridge University Press, Boston, MA (1992).
12. J. B. Liu, "Choice of the best band combination of hyper spectral data," see http://www.gisdevelopment.net/aars/acrs/1999/ps6/ps61226.shtml.
13. S. C. Pei and I. K. Tam, "Effective color interpolation in CCD color filter array using signal correlation," *Proc. Intl. Conf. Image Process.* **3**, 488–491 (2000).

14. M. Amadasun and R. King, ''Texture features corresponding to textural properties,'' *IEEE Trans. Syst. Man Cybern.* **19**, 1264–1274 (1989).
15. R. S. Berns, ''Challenges for color science in multimedia imaging,'' in *Color Imaging: Vision and Technology*, L. W. MacDonald and M. R. Luo, eds., pp. 99–128, John Wiley and Sons, Ltd., Chichester, United Kingdom (1999).
16. E. D. Montag and R. S. Berns, ''Visual determination of hue suprathreshold color-difference tolerances using CRT-generated stimuli,'' *Color Res. Appl.* **24**(3), 164–176 (1999).
17. J. H. Xin, C. C. Lam, and M. R. Luo, ''Investigation of parametric effects using medium colour-difference pairs,'' *Color Res. Appl.* **26**(5), 376–383 (2001).
18. G. Hong and R. Luo, ''Perceptually based colour difference for complex images,'' *AIC01 Conf.* Rochester, NY, June 2001.
19. R. S. Berns, R. J. Motta, and M. E. Gorzynski, ''Part I: Theory and practice, Colour research and application,'' *Color Res. Appl.* **18**(3), 299–314 (1993).
20. S. Ishihara, *Series of Plates Designed as a Test for Color-Blindness*, Kanehara Shuppan Co., Tokyo (1976).
21. D. C. Rich, D. L. Alston, and L. H. Allen, ''Psychopsysical verification of the accuracy of color and color-difference simulations of surface samples on a CRT display,'' *Color Res. Appl.* **17**(1), 45–56 (1992).

John H. Xin graduated with a PhD from the University of Leeds, United Kingdom, in 1989. Thereafter, he joined the multinational textile company Coats Viyella, United Kingdom, as a technologist in the color section of the research and development department. He joined University of Derby, United Kingdom, as a project coordinator for the development of a new generation computer color management and color quality control system in 1994. He joined Institute of Textiles and Clothing, The Hong Kong Polytechnic University, in 1996, and is currently an associate professor. His research interests are in the areas of color management, digital color communication and reproduction, and psychological aspects of color. He is a Charted Colourist, awarded by the Society of Dyers and Colourists, United Kingdom.

Hui-Liang Shen received his BSc and PhD degrees in information and electronic engineering from Zhejiang University, China, in 1996 and 2002, respectively. He is currently a research associate in the Institute of Textiles and Clothing, The Hong Kong Polytechnic University. His research interests are color imaging, computer vision, and image processing.